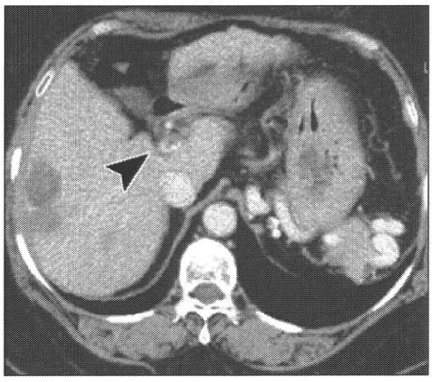

A

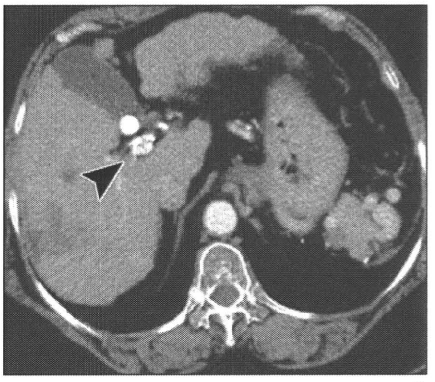

B

Fig. 3—Improvement of portal blood flow in 72-year-old woman with portal vein (PV) tumor thrombosis who underwent hepatic arterial infusion chemotherapy after radiofrequency ablation.
A, CT scan obtained before patient underwent combined therapy shows lumen of portal major trunk is occluded by PV tumor thrombosis (*arrowhead*).
B, CT scan obtained after patient received combined therapy shows blood flow of portal major trunk (*arrowhead*) has recovered.

treatment by RFA and HAI chemotherapy for the treatment of huge HCC and PV tumor thrombosis. This treatment appears safe and beneficial for patients showing huge HCC with PV tumor thrombosis, improving prognosis.

References

1. Fukuda S, Okuda K, Imamura M, Imamura I, Eriguchi N, Aoyagi S. Surgical resection combined with chemotherapy for advanced hepatocellular carcinoma with tumor thrombus: report of 19 cases. *Surgery* 2002; 131:300–310
2. Inoue Y, Hasegawa K, Ishizawa T, et al. Is there any difference in survival according to the portal tumor thrombectomy method in patients with hepatocellular carcinoma? *Surgery* 2009; 145:9–19
3. Chung JW, Park JH, Han JK, Choi BI, Han MC. Hepatocellular carcinoma and portal vein invasion: result of treatment with transcatheter oily chemoembolization. *AJR* 1995; 165:315–321
4. Ishida K, Hirooka M, Hiraoka A, et al. Treatment of hepatocellular carcinoma using arterial chemoembolization with degradable starch microspheres and continuous arterial infusion of 5-fluorouracil. *Jpn J Clin Oncol* 2008; 38:596–603
5. Sakon M, Nagano H, Dono K, et al. Combined intraarterial 5-fluorouracil and subcutaneous interferon-alpha therapy for advanced hepatocellular carcinoma with tumor thrombi in the major portal branches. *Cancer* 2002; 94:435–442
6. Obi S, Yoshida H, Toune R, et al. Combination therapy of intra-arterial 5-fluorouracil and systemic interferon alpha for advanced hepatocellular carcinoma with portal venous invasion. *Cancer* 2006; 106:1990–1997
7. Ando E, Yamashita F, Tanaka M, et al. A novel chemotherapy for advanced hepatocellular carcinoma with tumor thrombosis of the main trunk of the portal vein. *Cancer* 1997; 79:1890–1896
8. Nagano H, Miyamoto A, Wada H, et al. Interferon alpha and 5-fluorouracil combination therapy after palliative hepatic resection in patients with advanced hepatocellular carcinoma, portal venous tumor thrombus in the major trunk, and multiple nodules. *Cancer* 2007; 110:2493–2501
9. Takaki H, Yamakado K, Uraki J, et al. Radiofrequency ablation combined with chemoembolization for the treatment of hepatocellular carcinomas larger than 5 cm. *J Vasc Interv Radiol* 2009; 20:217–224
10. Chen MH, Yang W, Zou MW, Solbiati L, Liu JB, Dai Y. Large liver tumors: protocol for radiofrequency ablation and its clinical application in 110 patients—mathematic model, overlapping mode, and electrode placement process. *Radiology* 2004; 232:260–271
11. Giorgio A, Stefano G, Sarno A, et al. Radiofrequency ablation of hepatocellular carcinoma extended into the portal vein: preliminary results. *J Ultrasound* (in press)
12. Zheng RQ, Kudo M, Minami Y, Inui K, Chung H. Stage IV hepatocellular carcinoma with portal venous tumor thrombus: complete response after combined therapy of repeated arterial chemoembolization and radiofrequency ablation. *J Gastroenterol* 2003; 38:406–409
13. Stoesslein F, Ditscherlein G, Romaniuk PA. Experimental studies on new liquid embolization mixtures (Histoacryl-Lipiodol, Histoacryl-Pantopaque). *Cardiovasc Intervent Radiol* 1982; 5: 264–267
14. Uehara T, Hirooka M, Ishida K, et al. Percutaneous ultrasound-guided radiofrequency ablation of hepatocellular carcinoma used with artificially-induced pleural effusion and ascites. *J Gastroenterol* 2007; 42:306–311
15. Oken MM, Creech RH, Tormey DC, et al. Toxicity and response criteria of the Eastern Cooperative Oncology Group. *Am J Clin Oncol* 1982; 5: 649–655
16. Kudo M, Chung H, Haji S, et al. Validation of a new prognostic staging system for hepatocellular carcinoma: the JIS score compared with the CLIP score. *Hepatology* 2004; 40:1396–1405
17. Takizawa D, Kakizaki S, Sohara N, et al. Hepatocellular carcinoma with portal vein tumor thrombosis: clinical characteristics, prognosis, and patient survival analysis. *Dig Dis Sci* 2007; 52:3290–3295
18. Miyama S, Matsui O, Taki K, et al. Extrahepatic blood supply to hepatocellular carcinoma: angiographic demonstration and transcatheter arterial chemoembolization. *Cardiovasc Intervent Radiol* 2006; 29:39–48
19. Park SI, Lee DY, Won JY, Lee JT. Extrahepatic collateral supply of hepatocellular carcinoma by the intercostal artery. *J Vasc Interv Radiol* 2003; 14:461–468
20. Riaz A, Kulik L, Lewandowski RJ, et al. Radiologic–pathologic correlation of hepatocellular carcinoma treated with internal radiation using yttrium-90 microspheres. *Hepatology* 2009; 49: 1185–1193
21. Livraghi T, Grigioni W, Mazziotti A, Sangalli G, Vettori C. Percutaneous alcohol injection of portal thrombosis in hepatocellular carcinoma: a new possible treatment. *Tumori* 1990; 76:394–397

Contrast-Enhanced Sonography With Abdominal Virtual Sonography in Monitoring Radiofrequency Ablation of Hepatocellular Carcinoma

Yoshiyasu Kisaka, MD, Masashi Hirooka, MD, Yohei Koizumi, MD, Masanori Abe, MD, Bunzo Matsuura, MD, Yoichi Hiasa, MD, Morikazu Onji, MD

Department of Gastroenterology and Metabology, Ehime University Graduate School of Medicine, 454 Shitsukawa, Toon, Ehime 791-0295, Japan

Received 26 February 2009; accepted 28 October 2009

ABSTRACT: *Background.* Contrast-enhanced CT is regarded as the gold standard for monitoring radiofrequency ablation (RFA) of hepatocellular carcinoma (HCC). Recently, 3-dimensional volume data from CT have been used to create cross-sectional multiplanar reconstruction images. Using this technique, we can reconstruct 2-dimensional CT images identical in orientation to ultrasound (US) images, which we call virtual sonographic (VUS) images. The present prospective randomized control trial compared the number of CT scans needed to assess the efficacy of RFA of HCC using VUS-contrast-enhanced ultrasonography (CEUS) versus CT.

Method. Subjects comprised 50 patients (50 HCCs) treated with US-guided RFA between May 2005 and August 2006, randomized to undergo assessment by CT (Group 1; 25 HCC nodules) or VUS-CEUS (Group 2; 25 HCC nodules). All patients were followed for 1 year. Primary endpoint was whether the number of CT scans could be reduced using VUS-CEUS.

Result. Mean number of CT scans required was 1.64 ± 0.7 in Group 1 and 1.1 ± 0.2 in Group 2 ($p < 0.001$).

Conclusion. VUS-CEUS can be used to assess the efficacy of HCC of RFA, with the potential to reduce the number of CT scans required for that purpose. © 2009 Wiley Periodicals, Inc. *J Clin Ultrasound* **38**:138–144, 2010; Published online in Wiley InterScience (www.interscience.wiley.com). DOI: 10.1002/jcu.20654

Keywords: radiofrequency ablation; therapeutic response; virtual ultrasonography; contrast-enhanced ultrasonography; liver; hepatocellular carcinoma (HCC)

The incidence of hepatocellular carcinoma (HCC) is increasing worldwide.[1–3] Unlike other solid tumors, surgical resection plays a limited role in the treatment of HCC, as underlying cirrhosis or tumor multicentricity often contraindicates surgery.[4–6] Furthermore, HCC recurs frequently, even after curative resection.[7] Therapies such as percutaneous ethanol injection,[8–10] microwave coagulation therapy,[11,12] and radiofrequency ablation (RFA) are thus widely used in the treatment of unresectable HCC.[13–16]

RFA is frequently performed in Japan and has a higher rate of complete necrosis than other ablative procedures. For the treatment to be complete, the entire tumor must be ablated with a sufficient rim (≥5.0 mm) of noncancerous hepatic parenchyma.

Contrast-enhanced CT is the most commonly used modality for assessing the efficacy of RFA, as the ablated margin can be determined by CT both before and after RFA.[17,18] In addition, the exact ablated margin can be evaluated by injecting iodized oil (Lipiodol; Bayer, Osaka, Japan) in the tumor before RFA to delineate it subsequently (Figure 1A). CT is 1 of the most commonly used modalities for assessing the margins of the ablated volume, but it is expensive and involves potentially problematic radiation exposure.[19] Contrast-enhanced ultrasonography

Correspondence to: Y. Hiasa

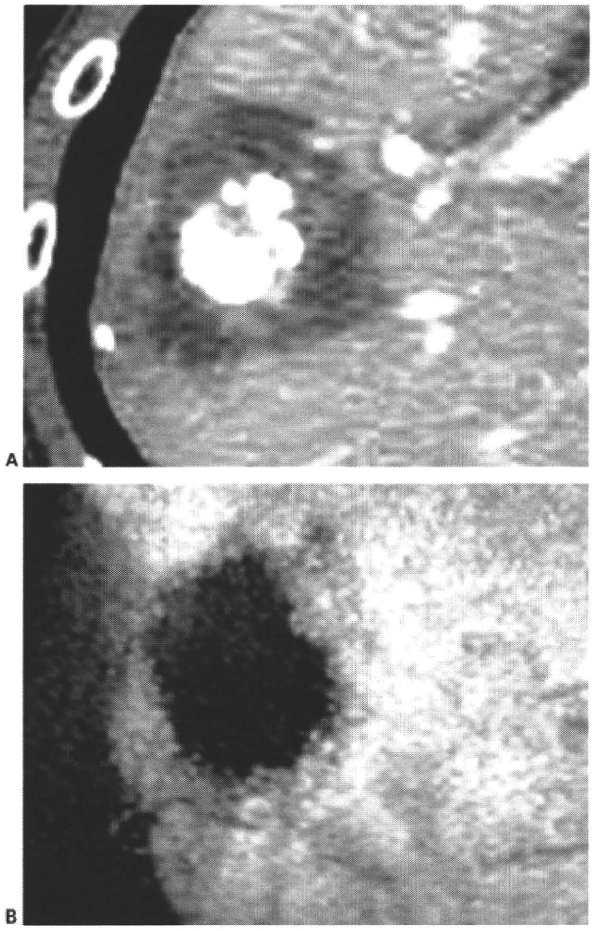

FIGURE 1. A: Post-RFA CT shows that the low-density area is larger than the ablated tumor into which iodized oil had been injected prior to RFA. The ablated margin was easily assessed, due to identification of the ablated tumor. B: In the postvascular phase on post-RFA CEUS, the ablated area appears as a homogenous unenhanced area. Ablated margins are difficult to evaluate because of the difficulty in distinguishing between ablated tumor and ablated nontumoral tissue.

(CEUS) has been reported as a useful procedure to assess the efficacy of HCC of RFA but still cannot accurately assess the ablated margins.[20]

Recently, 3-dimensional (3D) volume data from CT have been used to make cross-sectional multiplanar reconstruction images. Applying this technique, we have developed software that can reconstruct 2-dimensional CT scans identical in orientation to ultrasound scans (Virtual Place Advance software; AZE, Tokyo, Japan). We have called this technique virtual sonography (VUS).[21,22] Following RFA, the ablated margin can be assessed by comparing the VUS image of the tumor before RFA with the CEUS image showing the ablated area after RFA (VUS-CEUS) (Figure 2).

Sometimes more than 2 RFA sessions are required to ablate a HCC with a sufficient margin. In such cases, the number of CT scans required is equal to the number of sessions of RFA (Figure 3).

We therefore designed a new assessment of RFA using VUS-CEUS in replacement of CT (Figure 4). We have previously reported a retrospective study in which use of VUS-CEUS reduced the number of CT scans needed.[23] The present randomized control trial prospectively investigates the potential decrease in number of CT scans needed to assess the efficacy of RFA when VUS-CEUS is used.

PATIENTS AND METHODS

Eligibility Criteria

This study was approved by the ethics committee of the Ehime University Hospital. Between May 2005 and August 2006, a total of 50 HCCs in 50 patients were treated with US-guided percutaneous RFA. These patients were enrolled in the study after providing informed consent. All patients had to meet the following criteria for treatment with RFA: single nodular HCC $\leq$5 cm in maximum diameter; $\leq$3 lesions, each $\leq$3 cm in diameter; absence of portal venous thrombosis or extrahepatic metastases; Child-Pugh class A or B liver cirrhosis; prothrombin time >50%; and platelet count >50,000/μl. The diagnosis of HCC was confirmed by typical imaging findings, including high attenuation on CT during hepatic arteriography, and perfusion defect on CT during arterial portography. For patients with typical findings on CT during hepatic arteriography and CT during arterial portography, needle biopsy was not done.

RFA Technique

Before ablation, local anesthesia was obtained by injecting 5 ml of 1% lidocaine through the skin into the peritoneum along a predetermined puncture line. We then inserted a 20-cm-long, 17-gauge radiofrequency electrode equipped with a 2.0- or 3.0-cm-long exposed metallic tip (Cool tip; Radionics, Burlington, MA) into the tumor. If the nodule was obscured by the lungs, 500 ml saline was injected into the right pleural cavity.[24]

CT (GE Medical System, Milwaukee, WI) was performed using a Light Speed Ultra 16 scanner before RFA and at 3–5 days after treatment. Scanning parameters were as follows: 120 kVp; 175–189 mAs; 5-mm slice thickness; and table speed of 18 mm/s (pitch 0.98°) during a single

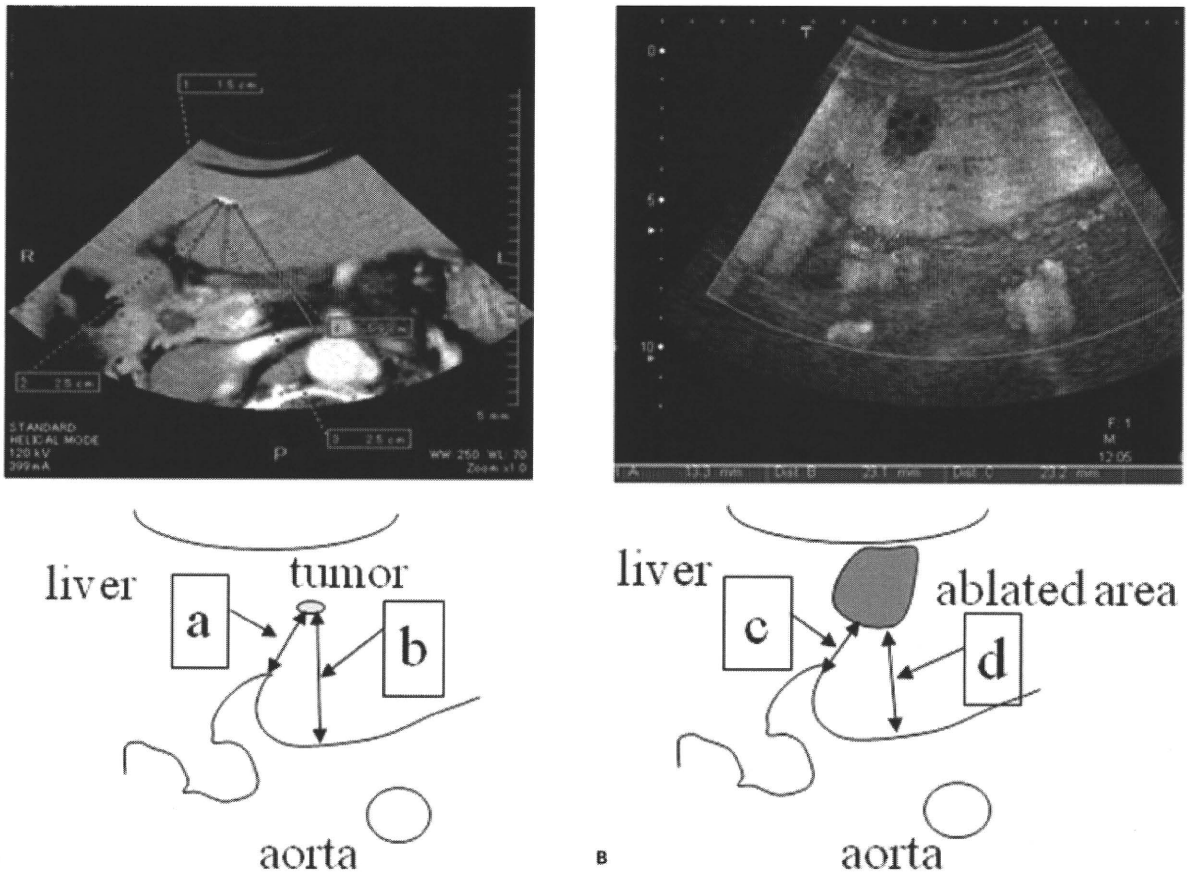

FIGURE 2. A: Assessing efficacy of RFA with VUS-CEUS. VUS shows the tumor before RFA. B: After RFA. Five minutes after injecting contrast agent (Levovist), CEUS shows the ablated area as a homogeneous unenhanced area. The difference between distances measured on VUS and on CEUS (for example, a-c, b-d in A and B) was defined as the safety margin of ablation.

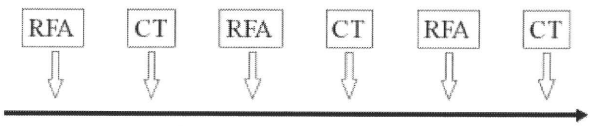

FIGURE 3. Timeline for assessing efficacy of RFA of HCC using CT (for example, in this case after 3 RFA sessions). CT was performed 3–5 days after each RFA session. The number of CT scans is equal to the number of RFA sessions.

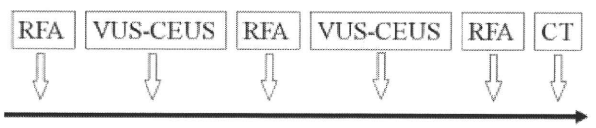

FIGURE 4. Timeline for assessing efficacy of RFA of HCC using VUS-CEUS instead of CT. VUS-CEUS was performed 3 days after each RFA session.

breath-hold helical acquisition of 7.7–10.5 seconds.

CEUS was performed 3 days after RFA using an Aplio XV system (Toshiba, Tokyo, Japan) equipped with a 4-MHz convex array transducer. The focal zone was set at the deeper margin of the tumor. Acoustic power was set at the default setting (mechanical index, 1.3–1.4). Advanced dynamic flow with a wideband Doppler technique was used, and the dynamic range for advanced dynamic flow was 40 dB. Gain was adjusted to optimize image quality in each patient. The US contrast agent used in this study was SH U 508A (Levovist; Bayer) at a dose of 300 mg/dl. The contrast was injected manually through a 20-gauge cannula into an antecubital vein at 1 ml/s. We assessed vascularity within the ablated area by means of continuous scanning at a frame rate of 5 frames/s for 10–30 seconds after injection. The ablated area was again evaluated 5 minutes after injection of US contrast medium. In this postvascular phase, the ablated area was visualized as a homogeneous nonenhanced area. Distinguishing between the ablated tumor and ablated parenchymal tissue was thus difficult. To identify the region of ablated tumor, VUS was used. For synthesis of VUS images, VUS images were generated with the software from the 3D CT volume data. It is to be noted that reconstructed VUS images are not sonograms but CT generated images that match the actual sonograms in orientation.

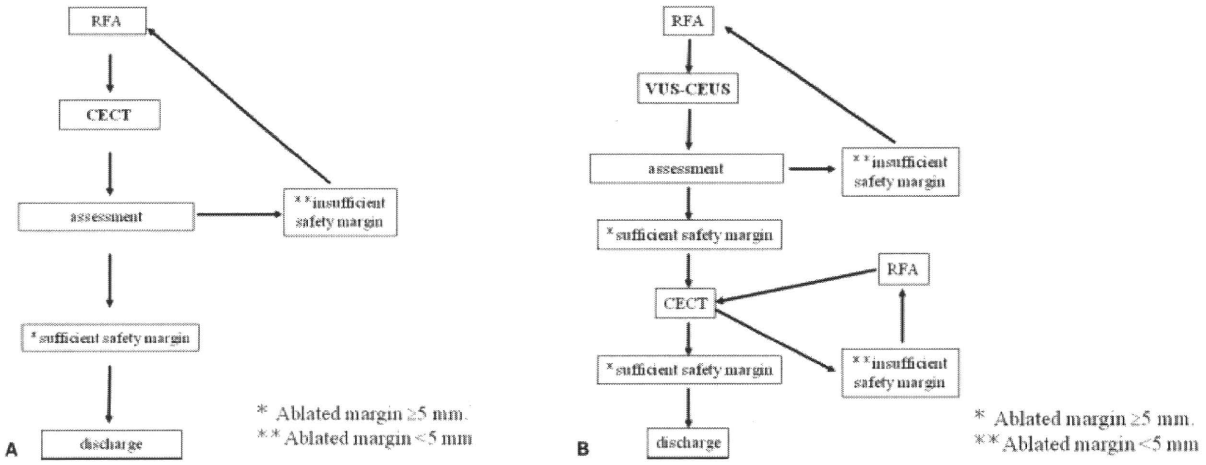

FIGURE 5. A: Assessment of efficacy of RFA of HCC with CT. If the margin is insufficient, RFA is performed again. The ablated margin is then assessed again by CT. B: Assessment of efficacy of RFA using VUS-CEUS. If the margin is insufficient, RFA is repeated. The safety margin is then assessed again by VUS-CEUS. This is continued until complete tumor ablation has been achieved. We then confirm the safety margin by CT. If the margin is insufficient, RFA is performed again. After additional RFA, efficacy is again assessed by CT.

We used anatomical landmarks to objectively measure the margins of the ablated volume. On VUS, position of the tumor was identified by measuring distance from the edge of the tumor to the anatomic landmarks (ie, surrounding organs, vessels, or edge of the liver). The same distances were also measured on CEUS scans. If the distances between the margins of the lesion and the anatomical landmarks measured on CEUS were smaller than those measured on VUS, the ablated volume was considered sufficient (Figure 2). For treatment to be complete, the entire tumor had to be ablated along with a sufficient rim of at least 5.0 mm of hepatic parenchyma. When tumors were located close (<5 mm) to the liver surface or major vessels, treatment to the adjacent parenchyma was regarded as complete ablation.

Study Design

Subjects were randomized into 2 groups of 25 cases each by computer-generated allocation with instructions in sealed envelopes to obtain 1 group of HCC treated with RFA and evaluated only by CT (Group 1) and another 1 (Group 2) evaluated with VUS-CEUS. In Group 1, efficacy of RFA was evaluated by CT as the gold standard (Figure 5A). In Group 2, VUS-CEUS was performed 3 days after each session of RFA. We performed evaluations 3 days after RFA because we wanted to evaluate not only the ablated area, but also remaining vascularity of the tumor. Vascularity could not be evaluated at 1 or 2 days after RFA, as high echogenicity persists for several hours after RFA treatment, and hypervascularity due to inflammation around the ablated area persists for 1 or 2 days. When the therapeutic effect was judged sufficient on VUS-CEUS, RFA was performed again. Three days after a second RFA, efficacy was again evaluated by VUS-CEUS. When the volume of the necrotic area was sufficient, as determined by VUS-CEUS, the lesion was evaluated by CT. If therapy was incomplete, a repeat RFA was performed. If the ablated margin was sufficient, treatment was considered complete (Figure 5B). The primary endpoint of the study was the number of CT scans needed to confirm successful RFA, and secondary endpoints were the rate of local recurrence, incidence of adverse events, and the number of treatment sessions. After treatment with RFA, serum α-fetoprotein, lectin-reactive α-fetoprotein, and plasma des-γ-carboxy-prothrombin levels were measured monthly; dynamic CT was performed after 3, 6, and 12 months, and US was performed every 3 months. Local recurrence was defined as the appearance of viable cancer adjacent to the original lesion. All patients were followed for 1 year. Major complications were defined as hemorrhage, pleural effusion requiring drainage, hepatic infarction, pneumothorax, hemothorax, bile peritonitis, liver abscess, and gastrointestinal perforation. Other complications were defined as minor complications.

Statistical Analysis

Data are expressed as mean ± SD. We calculated that a sample size of ≥22 HCCs in each group

(total, 44 HCCs) would be needed to detect a significant difference in the number of CT scans with 5% type I error and 80% power using Student's t test. This calculation was performed prior to initiation of the study. Values of $p < 0.05$ were considered to represent a statistically significant difference. SPSS version 15.0 software (SPSS, Chicago, IL) was used for all analyses.

RESULTS

The clinical characteristics of patients (age, sex, TNM stage, tumor size, localization, Child-Pugh status) did not differ significantly between the 2 groups (Table 1). Mean number of CT scans was 1.6 ± 0.7 (range, 1–4) in Group 1 and 1.1 ± 0.2 (range, 1–2) in Group 2 ($p < 0.01$). The mean number of RFA sessions was 1.6 ± 0.7 (range, 1–4) in Group 1 and 1.8 ± 0.9 (range, 1–4) in Group 2 with no significant differences between the 2 groups. Local recurrence rate at 1 year occurred in 1 of 25 cases (4.0%) in Group 1 and 2 of 25 nodules (8.0%) in Group 2. No major complication occurred after RFA in either group. Minor complications (predominantly elevated temperature) were observed in about 50% of patients (16 patients in Group 1; 17 patients in Group 2). No patient showed reduced liver function, including changes in prothrombin time, cholinesterase, albumin, or total protein. Two of 25 nodules in Group 2 were evaluated as showing sufficient safety margin by VUS-CEUS but were evaluated as having insufficient safety margin by CT.

TABLE 1
Clinical Characteristics of Patients in the CT Group (Group 1) and VUS-CEUS Group (Group 2)

	Group 1 (N = 25)	Group 2 (N = 25)	p value
Sex (M:F)	22:3	16:9	NS
Age (yr)	66.1 ± 7.1	67.0 ± 8.9	NS
TNM stage (1:2:3)	6:12:7	5:10:10	NS
Tumor localization (S1: left: middle: right anterior: right posterior)	1:4:4:9:7	0:6:3:9:7	NS
Tumor size (mm)	17.2 ± 8.9	17.0 ± 6.5	NS
Child-Pugh-classification (A:B)	21:4	19:6	NS

Abbreviation: NS, not significant.

DISCUSSION

Determining whether the tumor was ablated completely and whether sufficient ablated margins were achieved is critical for local control of HCC.[20,25–29] CEUS has recently been reported as a useful procedure to assess the efficacy of RFA of HCC.[20] Evaluation of the vascularity of residual tumors with CEUS is comparable to CT, and CEUS can be used in patients allergic to iodine. Patients with renal failure may also be good candidates for CEUS. Moreover, this approach is less costly and does not involve any exposure to radiation.

On CEUS the ablated area is visualized as a homogeneous nonenhanced area in the postvascular phase (Figure 1B), and identifying the exact margin of the ablated volume is difficult due to the inability to distinguish between ablated tumor and ablated parenchymal tissue.[20] We thus used VUS imaging reconstructed from 3D CT volume data. This allows assessment of the ablated margin by comparing between VUS images depicting location of the tumor before RFA and CEUS images depicting the ablated area after RFA. We have already reported that compared with the gold standard of CT, this method had a sensitivity, specificity, positive predictive value, negative predictive value, and diagnostic accuracy of 92.3%, 76.9%, 80%, 90.9% and 84.6%, respectively.[23] As a result, the number of CT scans required after RFA can be reduced.[23]

The present randomized control trial compared the number of CT scans required to assess the efficacy of RFA between a group using CT alone and a group using VUS-CEUS with CT. In this study, 2 lesions whose RFA was evaluated by VUS-CEUS (Group 2) were considered as completely ablated, but the ablated area was actually insufficient according to CT. Those 2 nodules were located where no obvious anatomical landmarks were present, so a pair of identical VUS and CEUS scans could not be generated and ablated tumor tissue could not be unequivocally identified. Success of RFA of other nodules could be assessed by VUS-CEUS. Rates of HCC recurrence did not differ significantly between Groups 1 and 2. This means that evaluating the efficacy of RFA using VUS-CEUS allows accurate determination of ablated margins.

In this study, to avoid disadvantaging Group 2 patients, all HCC nodules in Group 2 treated successfully according to VUS-CEUS were also checked by CT before discharge from hospital. Indeed, recurrence and complication rates did not differ significantly between the 2 groups. Assessing the success of RFA by VUS-CEUS is a promising method and the number of CT scans was significantly decreased using VUS-CEUS. This may contribute to reducing the costs, X-ray

exposure, and occasional risk associated with contrast agents for CT.

When this study was started, the contrast agent SH U 508A (Levovist) was the only agent available for use in Japan. However, perflubutane gas is now available as a new contrast agent (Sonazoid; Daiichi-Sankyo, Tokyo, Japan). Perflubutane gas provides a parenchyma-specific contrast image based on accumulation in Kupffer cells. The efficacy of using this new contrast agent should be confirmed using the same protocol.

In conclusion, use of VUS-CEUS could decrease the number of CT scans required to assess success of RFA of HCC, without increasing the risk of local recurrence or decreased liver function.

REFERENCES

1. El Serag HB, Mason AC. Rising incidence of hepatocellular carcinoma in the United States. N Engl J Med 1999;340:745.
2. Taylor Robinson SD, Foster GR, Arora S, et al. Increase in primary liver cancer in the UK, 1989–94. Lancet 1997;350:1142.
3. Okuda K, Okuda H. Primary liver carcinoma. In: McIntyre N, Benhamou T, Bircher J, editors. Oxford text book of clinical hepatology. Volume 2. Oxford, England: Oxford University Press; 1991, p 1019.
4. Bruix J, Sherman M, Llovert JM, et al. EASL Panel of Experts on HCC. Clinical management of hepatocellular carcinoma. Conclusion of the Barcelona-2000 EASL Conference European Association for the Study of the Liver. J Hepatol 2001;35:421.
5. Ryder S D. Guidelines for the diagnosis and treatment of hepatocellular carcinoma (HCC) in adults. Gut 2003;52:iii1.
6. Llovet JM, Burroughs A, Bruix J. Hepatocellular carcinoma. Lancet 2003;362:1907.
7. Balsells J, Charco R, Lazaro JL, et al. Resection of hepatocellular carcinoma in patients with cirrhosis. Br J Surg 1996;83:758.
8. Akamatsu K, Miyauchi S, Itoh Y, et al. Development and evaluation of a needle for percutaneous ethanol injection therapy. Radiology 1993;186:284.
9. Shiina S, Tagawa K, Unuma T, et al. Percutaneous ethanol injection therapy for hepatocellular carcinoma. A histopathologic study. Cancer 1991;68: 1524.
10. Livraghi T, Giorgio A, Marin G, et al. Hepatocellular carcinoma and cirrhosis in 746 patients: long-term results of percutaneous ethanol injection. Radiology 1995;197:101.
11. Seki T, Wakabayashi M, Nakagawa T, et al. Ultrasonically guided percutaneous microwave coagulation therapy for small hepatocellular carcinoma. Cancer 1994;74:817.
12. Murakami R, Yoshimatsu S, Yamashita Y, et al. Treatment of hepatocellular carcinoma: value of percutaneous microwave coagulation. Am J Roentgenol 1995;164:1159.
13. Rossi S, Buscarini E, Garbagnati F, et al. Percutaneous treatment of small hepatic tumours by an expandable RF needle electrode. Am J Roentgenol 1998;170:1015.
14. Goldberg SN, Gazelle GS, Solbiati L, et al. Ablation of liver tumours using percutaneous RF therapy. Am J Roentgenol 1998;170:1023.
15. Tateishi R, Shiina S, Teratani T, et al. Percutaneous radiofrequency ablation for hepatocellular carcinoma. An analysis of 1000 cases. Cancer 2005; 103:1201.
16. Horiike N, Iuchi H, Ninomiya T. Influencing factors for recurrence of hepatocellular carcinoma treated with radiofrequency ablation. Oncol Rep 2002;9:1059.
17. Solbiati L, Ierace T, Goldberg SN, et al. Percutaneous US-guided radio-frequency tissue ablation of liver metastases: treatment and follow-up in 16 patients. Radiology 1997;202:195.
18. Livraghi T, Goldberg SN, Monti F, et al. Saline-enhanced radio-frequency tissue ablation in the treatment of liver metastases. Radiology 1997;202: 582.
19. Berrington de Gonza'lez A, Darby S. Risk of from diagnostic X-rays; estimates for the UK and 14 other countries. Lancet 2004;363:345.
20. Shimizu M, Iijima H, Horibe T, et al. Usefulness of contrast enhanced ultrasonography with a new contrast mode, agent detection imaging, in evaluating therapeutic response in hepatocellular carcinoma treated with radio-frequency ablation therapy. Hepatol Res 2004;29:235.
21. Hirooka M, Iuchi H, Kurose K, et al. Abdominal virtual ultrasonographic images reconstructed by multi-detector row helical computed tomography. Eur J Radiol 2005;53:312.
22. Hirooka M, Iuchi H, Kumagi T, et al. Radiofrequency ablation using virtual ultrasonography of hepatocellular carcinoma visualized on CT not on conventional ultrasonography. Am J Roentgenol 2006;186:S255.
23. Kisaka Y, Hirooka M, Kumagi T, et al. Usefulness of contrast enhanced ultrasonography with abdominal virtual ultrasonography in assessing therapeutic response in hepatocellular carcinoma treated with radiofrequency ablation. Liver Int 2006;26:1241.
24. Koda M, Ueki M, Maeda Y, et al. Percutaneous sonographically guided radiofrequency ablation with artificial pleural effusion for hepatocellular carcinoma located under the diaphragm. Am J Roentgenol 2004;183:583.
25. Kim YS, Rhim H, Cho OK, et al. Intrahepatic recurrence after percutaneous radiofrequency ablation of hepatocellular carcinoma; analysis of the pattern and risk factor. Eur J Radiol 2006;59: 432.

26. Choi BI, Kim HC, Han JK, et al. Therapeutic effect of transcatheter oily chemoembolization therapy for encapsulated nodular hepatocellular carcinoma. CT and pathologic findings. Radiology 1992; 182:709.
27. Gazelle GS, Goldberg SN, Solbiati L, et al. Tumour ablation with radio-frequency energy. Radiology 2000;217:633.
28. Yamamoto K, Shiraki K, Nakanishi S, et al. 1.5 Harmonic imaging sonography with microbubble contrast agent improve characterization of hepatocellular carcinoma. World J Gastroenterol 2005;11: 5607.
29. Dutcher JP, Haney PJ, Whitley NO, et al. Ethiodized oil emulsion 13 in computed tomography of hepatoma. J Clin Oncol 1984;2:118.

JOURNAL OF VIRAL HEPATITIS
JVH

Journal of Viral Hepatitis, 2010 doi:10.1111/j.1365-2893.2010.01320.x

Safety and immunogenicity of hepatitis B surface antigen-pulsed dendritic cells in patients with chronic hepatitis B

S. M. F. Akbar,[1,2] S. Furukawa,[1] N. Horiike,[1] M. Abe,[1] Y. Hiasa[1] and M. Onji[1] [1]*Department of Medical Sciences, Toshiba General Hospital, Tokyo, Japan; and* [2]*Department of Gastroenterology and Metabology, Ehime University Graduate School of Medicine, Ehime Japan*

Received January 2010; accepted for publication March 2010

SUMMARY. The immune modulator capacity of antigen-pulsed dendritic cells (DC) has been documented in patients with cancers and in animal models of chronic viral infections. Cancer antigen-pulsed DC are now used for treating patients with cancer. But viral antigen-pulsed DC are not used in chronic viral-infected patients because safety of antigen-pulsed DC has not been evaluated in these patients. DC were isolated from human peripheral blood mononuclear cells by culturing with human-grade granulocyte-macrophage colony stimulating factor and interleukin-4. Human blood DC were cultured with hepatitis B surface antigen (HBsAg) for 8 h to prepare HBsAg-pulsed DC. After immunogenicity assessment of HBsAg-pulsed DC *in vitro*, five million HBsAg-pulsed DC were administered intradermally to five patients with chronic hepatitis B (CHB) 1–3 times. HBsAg-pulsed DC were immunogenic in nature because they produced significantly higher levels of interleukin-12 and interferon-γ compared to unpulsed DC ($P < 0.05$). Also, HBsAg-pulsed DC induced proliferation of HBsAg-specific T lymphocytes *in vitro*. CHB patients injected with HBsAg-pulsed DC did not exhibit generalized inflammation, exacerbation of liver damage, abnormal kidney function, or features of autoimmunity. Administration of HBsAg-pulsed DC induced anti-HBs in two patients and HBsAg-specific cellular immunity in 1 patient. This is the first study about preparation of antigen-pulsed DC using human consumable materials for treating patients with CHB. Because HBsAg-pulsed DC were safe for all patients with CHB and had immune modulation capacity in some patients, phase I and phase II clinical trials with antigen-pulsed DC in CHB and other chronic infections are warranted.

Keywords: antigen-pulsed dendritic cells, chronic hepatitis B, dendritic cells, hepatitis B surface antigen, therapeutic vaccine.

INTRODUCTION

There is no curative therapy for patients with chronic hepatitis B (CHB). Antiviral drugs are recommended to patients with CHB to attain sustained control of replication of the hepatitis B virus (HBV) and minimize liver damage [1]. However, the therapeutic efficacy of antiviral agents in patients with CHB is not complete, as most studies have reported only intermediate outcomes. A well-designed study for a National Institutes of Health consensus development conference analysed all randomized clinical trials with antiviral drugs in patients with CHB from 1989 to 2008 [2]. Results showed that no single drug treatment improved clinical outcomes or all intermediate outcomes of CHB [2], although improvements of some intermediate outcomes have been seen. However, adverse events during antiviral treatment occurred in about 50% patients. These facts support the need for a new and innovative therapeutic strategy against CHB.

Chronic HBV infection represents a viral-mediated immunological disease. Although HBV is a noncytopathic virus, patients with CHB exhibit features of liver damage and associated complications. HBV-specific immune responses are narrowly focused and weak in most patients with CHB [3]. Recent studies have also shown that impaired HBV-specific immunity and exacerbated polyclonal immune responses are related to viral persistence and liver damage in patients with CHB [4]. On the other hand, effective control

Abbreviations: ALT, alanine aminotransferase; CHB, chronic hepatitis B; CHB, chronic hepatitis B; DC, dendritic cells; HBsAg, hepatitis B surface antigen; HBV, hepatitis B virus; PBMC, Peripheral blood mononuclear cells; PBS, phosphate-buffered saline.

Correspondence: Morikazu Onji, MD, PhD., Professor and Chairman, Department of Gastroenterology and Metabology, Ehime University Graduate School of Medicine, Toon city, Ehime 791-0295, Japan.
E-mail: onjimori@m.ehime-u.ac.jp
S. M. F. Akbar and S. Furukawa contributed equally to this study.

of HBV replication and liver damage are associated with strong HBV-specific immunity in these patients [5].

Taken together, restoration of HBV-specific immunity in patients with CHB may have some therapeutic potential. In fact, a new field of clinical application of vaccines containing hepatitis B surface antigen (HBsAg) has been initiated to restore HBsAg-specific immune responses in patients with CHB [6,7]. Although safer and cheaper than commercially available antiviral drugs, restoration of HBsAg-specific immunity was not attained in patients with CHB by vaccine therapy [8].

To develop a more potent regimen of antigen-specific immune therapy, the role of antigen-presenting dendritic cells (DC) in adaptive immunity has been examined. DC are responsible for processing and presenting antigens for induction of antigen-specific immune responses in normal conditions as well as in the immune tolerance state [9,10]. Studies have shown that the phenotypes and functions of DC are distorted in patients with CHB [11,12]. Accordingly, during vaccine therapy, HBsAg may not be properly processed by DC in patients with CHB to induce HBsAg-specific immune responses.

One way to circumvent this problem is to produce antigen-pulsed DC and use them as a vaccine [9,10]. In fact, cancer antigen-pulsed DC are widely used to induce cancer-specific immunity in patients with cancer [13]. However, antigen-pulsed DC have not been produced for human use in other patient groups, and almost nothing is known about their therapeutic use outside cancer.

In our study, human blood DC were cultured with human consumable HBsAg to prepare human-grade HBsAg-pulsed DC. The functions of HBsAg-pulsed DC were assessed *in vitro*. Finally, a pilot study was carried out in patients with CHB to evaluate the safety of HBsAg-pulsed DC. The induction of HBsAg-specific immunity by HBsAg-pulsed DC was also assessed in these patients.

MATERIALS AND METHODS

Clinical trial design and study population

The study was an open-label, phase-1 safety trial in patients with CHB. Five patients with CHB were enrolled in this study. Informed written consent has been obtained from each patient. The study has been performed according to the World Medical Association declaration of Helsinki, and the procedures have been approved by the Ethical Committee of Ehime University Graduate School of Medicine, Japan. Enrolled patients did not have serological markers of hepatitis A virus, hepatitis C virus, hepatitis E virus, or human immune deficiency virus at that time of trial start. The diagnosis of CHB was made from data on clinical and serological parameters. All subjects were positive for HBsAg, HBV DNA, and antibody to hepatitis core antibody in the sera. Two subjects (patients 1 and 2) were positive for hepatitis B e antigen, whereas three subjects (patients 3, 4, and 5) were positive for antibody to hepatitis B e antigen. Anti-HBs antibodies were not detected in any patient. In four patients, liver biopsy specimens were available to make a histological diagnosis (patients 1, 2, 3, and 5). All of them had moderate levels of hepatitis. Levels of fibrosis were mild in patients 1 and 2 and severe in patients 3 and 5. These patients were attending our university hospital for regular follow-up and treatment. The clinical profiles of patients before administration of HBsAg-pulsed DC are shown in Table 1. Levels of alanine aminotransferase (ALT) in the sera were elevated in three patients (patients 1, 2, and 5) and within normal limits in patients 3 and 4. No patient showed any feature of general inflammation (assessed from serum levels of C-reactive protein) or abnormal kidney function.

Isolation of DC from peripheral blood and loading of HBsAg in vitro

Isolation of human blood DC and production of HBsAg-pulsed DC were carried out as reported previously [14]. A special room was assigned for cell cultures, and DC were isolated from one person at a time. All reagents used for cell culture studies were free from endotoxin and toxoplasma. Peripheral blood mononuclear cells (PBMC) were isolated from freshly drawn heparinized whole blood, washed three times, and resuspended in RPMI 1640 (Nipro, Osaka, Japan) plus 10% autologous serum. DC were enriched from an adherent population of PBMC, as described previously [14]. PBMC were cultured in RPMI 1640 plus 10% autologous sera and human-grade granulocyte-macrophage stimulating factor (800 U/mL) and interleukin (IL)-4 (400 U/ml) (Pepro Tech EC Ltd., London, UK) for 7 days. DC were retrieved from the culture and washed three times with phosphate-buffered saline (PBS). The expressions of DC-related markers on human DC were checked by direct flow cytometry.

To produce HBsAg-pulsed DC, blood DC were cultured with a commercially available HB vaccine containing 10 μg of HBsAg (Heptavax-II, subtype adw, Banyu Pharmaceutical Co., Tokyo, Japan) for 8 hours. After the end of culture, DC were pelleted and washed five times in PBS. After the last wash, the final solutions were collected and preserved at −20 °C to assess if there was any free HBsAg in HBsAg-pulsed DC. As a control, human blood DC were cultured in RPMI 1640 plus autologous sera for 8 h.

Analyses of phenotype and functions of DC

The expression of HLA DR and CD86 on unpulsed DC and HBsAg-pulsed DC were assessed by direct flow cytometry using fluorescein isothiocyanate-conjugated monoclonal antibody to human HLA DR (Clone L243) and phycoerythrin-conjugated monoclonal antibody to human CD86 (clone 2331 [FUN-1]) (all from BD Pharmingen, San Jose,

Table 1 Clinical profiles of patients with chronic hepatitis B before administration of HBsAg-pulsed DC

	Patient no.				
	1	2	3	4	5
Age (years)	36	30	35	48	57
Sex	Male	Male	Male	Female	Male
Alanine aminotransferase (5–48 IU/L)*	169	83	35	31	95
Asparate aminotransferase (6–45 IU/L)	76	52	30	40	80
Prothrombin time (80–120%)	112.6	100	84	85.3	108.6
Creatinine (0.61–1.04 mg/dL)	0.6	0.7	0.6	0.6	0.9
Blood urea nitrogen (6–20 mg/dL)	8.0	12.0	11.0	11.0	14.0
C-reactive protein (<0.30 mg/dL)	0.04	0.05	0.03	0.03	0.04
Antinuclear antibody (<40)	–	–	–	–	–
Histology					
Activity	A2	A1	A2	ND	A2
Fibrosis	F1	F1	F3	ND	F3
HBV DNA (Log genomic equivalent)	7.2	7.5	<3.7	4.8	7.5
Hepatitis B surface antigen (IU/ml)	+	+	+	+	+
Hepatitis B e antigen (S/CO)	+	+	–	–	–
Antibody to hepatitis B e antigen	–	–	+	+	+
Antibody to hepatitis B core antigen	+	+	+	+	+
Antibody to hepatitis B surface antigen	–	–	–	–	–

HBV, hepatitis B virus.
*Levels in parenthesis indicate normal range.

CA, USA). Data acquisition and analysis were performed on fluorescein-activated cell sorter (Becton Dickinson Biosciences, San Jose, CA, USA) [14].

T-cell stimulatory capacity and HBsAg-specific proliferative capacity of DC were assessed in allogenic mixed leucocyte reaction and antigen-specific lymphoproliferative assays. Human blood DC were cultured with allogenic T cells, or autologous T cells were cultured with unpulsed or HBsAg-pulsed DC for 104 h, and then [^{3}H]-thymidine was added to the cultures. The cultures were done for an additional 16 h. The cultures were then harvested using a semiautomatic harvester, and the level of incorporation of [^{3}H]-thymidine was shown as counts per minute in a scintillation counter (Beckman LS 6500, Beckman Instruments, Inc., Fullerton, CA, USA) [14]. Data were also expressed as counts per minute or a stimulation index that was calculated by dividing the counts per minute in culture containing HBsAg-pulsed DC with that of unpulsed DC. A stimulation index >2.0 was considered a significant proliferation.

Levels of IL-12 and interferon (IFN)-γ in samples were measured by an enzyme-linked immunosorbent assay (ELISA) using commercial kit (BD Pharmingen).

Estimation of HBsAg and anti-HBs

To estimate levels of HBsAg and anti-HBs, samples were sent to commercial companies (Special Reference Laboratory, Osaka, Japan). The estimation was performed using the chemiluminescence enzyme immunoassay method. Detection limits of HBsAg and anti-HBs were 0.2 ng/mL and 3.0 mIU/mL, respectively. Some samples were sent to a second commercial company (Shikoku Chuken Co, Matsuyama, Japan) for further confirmation.

Immunization of CHB patients with HBsAg-pulsed DC

HBsAg-pulsed DC were suspended in PBS and placed in two syringes. In one syringe, 20 μL of PBS containing 2×10^5 HBsAg-pulsed DC was suspended. In a second syringe, 5 million HBsAg-pulsed DC were diluted in 250 μL of PBS. First, 2×10^5 HBsAg-pulsed DC in 20 μL of PBS were injected at the anterior part of forelimb of patients with CHB to see if there was any hypersensitivity reaction. After 15 minutes, patients were injected intradermally in the deltoid region with 5 million HBsAg-pulsed DC. The patients with CHB were allowed to rest for 30 min. They were then monitored periodically for temperature, pulse rate, blood pressure, and respiratory rate for the first 24 h. Blood was collected from all patients before immunization and at different times after immunization with HBsAg-pulsed DC. Parameters of generalized inflammation, liver function test, kidney function test, and autoantibodies were checked in all patients at different times after the administration of HBsAg-pulsed DC. Patients received 1, 2, or 3 injections over 4 months. The immunization schedule for each patient is shown in Fig. 1.

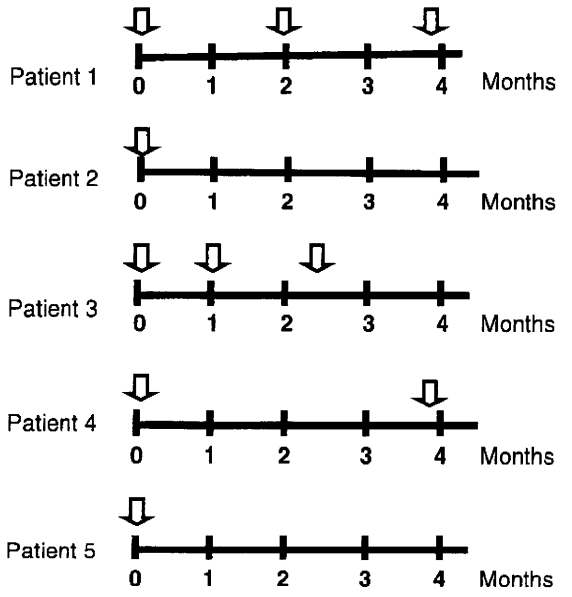

Fig. 1 Immunization schedule with HBsAg-pulsed DC in patients with chronic hepatitis B (CHB). HBsAg-pulsed DC were administered 1–3 times (arrows).

Statistical analysis

Values are represented as mean ± standard deviation (SD). Data were analysed by unpaired t tests if data were normally distributed and by Mann–Whitney rank-sum test if they were skewed. Differences were considered significant if $P < 0.05$.

RESULTS

Features of human blood DC

As a preliminary study, we first isolated DC from patients with CHB and pulsed with HBsAg, as described previously [15]. Flow cytometry analysis revealed that the frequencies of contaminating T lymphocytes (CD3-positive cells), B lymphocytes (CD19, 20, 21-positive cells), monocytes (CD14-positive cells), and natural killer cells (CD56-positive cells) were less than 5% of the total DC (data not shown). DC from patients with CHB expressed DC-related antigens, such as HLA-A, B, C, HLA DR, CD86, and CD40. A functional study showed that DC from patients with CHB stimulated allogenic T cells in a dose-dependent manner (Fig. 2).

Characterization of HBsAg-pulsed DC from patients with CHB

During preliminary experiments, we checked two features of HBsAg-pulsed DC for this clinical trial: (i) there should be no free HBsAg in HBsAg-pulsed DC and (ii) HBsAg-pulsed DC should be immunogenic in nature so that it can induce

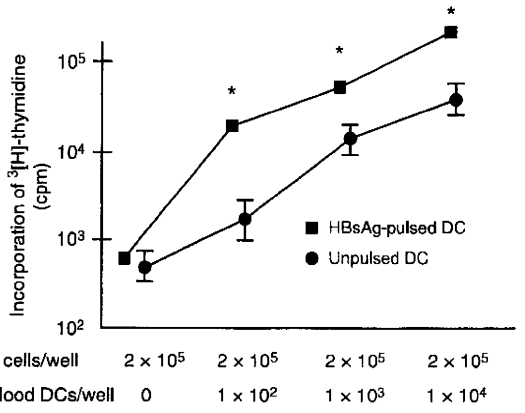

Fig. 2 DC from patients with chronic hepatitis B (CHB) stimulated allogenic T cells in a dose-dependent manner. However, HBsAg-pulsed DC had significantly higher capacities to induce blastogenesis of T cells compared with unpulsed DC. Data from 5 separate experiments are shown. cpm, counts per minute. *$P < 0.05$.

HBsAg-specific immune responses *in vivo*. No HBsAg was detected in the final wash solution of HBsAg-pulsed DC. Levels of IL-12 were significantly increased in culture containing HBsAg-pulsed DC from patients with CHB (156.2 ± 20.7 pg/mL) compared to unpulsed DC (29.2 ± 9.8 pg/mL) from patients with CHB ($P < 0.05$). Similarly, levels of IFN-γ were significantly increased in culture containing HBsAg-pulsed DC (232.4 ± 24.1 pg/mL) from patients with CHB compared to unpulsed DC (80.5 ± 12.9 pg/mL) from patients with CHB ($P < 0.05$). HBsAg-pulsed DC also induced significantly higher levels of blastogenesis of T cells compared to unpulsed DC (Fig. 2). Also, HBsAg-pulsed DC induced significant proliferation of HBsAg-specific T lymphocytes *in vitro* (data not shown). After confirming these points, we prepared HBsAg-pulsed DC for administration to patients with CHB.

Safety of HBsAg-pulsed DC in patients with CHB

No immediate or delayed inflammatory or allergic reaction was detected at the injection site of HBsAg-pulsed DC in any patient. No patient complained of any allergic reaction or fever after immunization with HBsAg-pulsed DC. Different parameters of blood biochemistry, liver and kidney functions, and immunological statuses of all patients with CHB were checked periodically, and data during follow-up period after the end of administration of HBsAg-pulsed DC in these patients have been shown in Table 2. There was no significant change in levels of C-reactive protein or other parameters of general features of inflammation because of administration of HBsAg-pulsed DC. In addition, parameters of kidney function were within normal ranges in all patients after the administration of HBsAg-pulsed DC. Features of autoimmunity or autoantibodies were not detected in any patient.

Table 2 Clinical profiles of patients with chronic hepatitis B during follow-up after completion of administration of HBsAg-pulsed DC

	Patient no. 1		Patient no. 2		Patient no. 3		Patient no. 4		Patient no. 5	
	1M*	3M	1M	3M	1M	3M	1M	3M	1M	3M
Alanine aminotransferase (5–48 IU/L)	171	147	57	36	37	30	43	41	109	72
Asparate aminotransferase (6–45 IU/L)	89	73	37	28	32	38	33	35	88	58
Prothrombin time (80–120%)	113.8	99.5	80.3	98.9	97	95	81.5	84.5	103.4	12.1
Creatinine (0.61–1.04 mg/dL)	0.7	0.7	0.7	0.7	0.6	0.6	0.6	0.6	0.9	1.0
Blood urea nitro- gen (6–20 mg/dL)	10	7	8	9	10	8	9	9	13	10
C-reactive protein (<0.30 mg/dL)	0.03	0.03	0.03	0.03	0.02	0.03	0.03	0.04	0.04	0.03
Antinuclear antibody (<40)	–	–	–	–	–	–	–	–	–	–
HBV DNA (Log genomic equivalent)	7.1	7.0	6.3	5.5	<3.7	<3.7	3.8	4.0	6.8	6.5

HBV, hepatitis B virus.
*Indicates month after end of last administration with hepatitis B surface antigen (HBsAg)-pulsed dendritic cells (DC). 1M: 1 month after completion of administration of HBsAg-pulsed DC, 3M; 3 months after completion of administration of HBsAg-pulsed DC.

Effect of HBsAg-pulsed DC on serum ALT levels

ALT levels just before the administration of HBsAg-pulsed DC are shown in Table 1. Because of the CHB, patients exhibited fluctuating ALT levels. The highest ALT level was <300 IU/L in all patients. There was no significant alteration in serum ALT levels because of administration of HBsAg-pulsed DC (Table 2).

Impact of HBsAg-pulsed DC as a therapeutic vaccine

The main aim of this study was to evaluate whether immunogenic HBsAg-pulsed DC can be prepared from DC of patients with CHB. The next goal was to assess whether administration of HBsAg-pulsed DC was safe. Although this study was not designed to assess the therapeutic potential of HBsAg-pulsed DC in patients with CHB, we checked levels of HBsAg, HBeAg negativity, and anti-HBe seroconversion in all patients. Administration of HBsAg-pulsed DC did not cause any major change in these parameters (data not shown). As shown in Table 2, the levels of HBV DNA were decreased slightly, but not significantly, because of administration of HBsAg-pulsed DC in these patients. Adverse effects were not detected in any patient. For example, three patients were anti-HBe positive, and the administration of HBsAg-pulsed DC did not cause reappearance of HBeAg in any patient.

Increased cytokine production by immunocytes of patients with CHB because of administration of HBsAg-pulsed DC

DC and T cells of patients with CHB were collected before and after the administration of HBsAg-pulsed DC and cultured in autologous mixed leucocyte reaction. Levels of IL-12 (before, 32.3 ± 5.2 pg/mL; after, 145 ± 9.2 pg/mL) and INF-γ (before, 21.7 ± 3.2 pg/mL; after, 154 ± 11.8 pg/mL) were significantly higher in culture supernatants after the administration of HBsAg-pulsed DC compared to before administration ($P < 0.05$).

HBsAg-specific immunity because of administration of HBsAg-pulsed DC

Administration of HBsAg-pulsed DC induced anti-HBs in two patients (patients 1 and 3). Anti-HBs were detected 1 month after HBsAg-pulsed DC administration in patient 1 and 2 months after HBsAg-pulsed DC administration in patient 3. Levels of anti-HBs increased progressively for 5 months in patient 1 and then started to decline. In contrast, levels of anti-HBs remained similar over time in patient 3 (Fig. 3).

HBsAg-specific cellular immunity in patient 1

HBsAg-specific T cells proliferation was not detected in any patient before study commencement. However, HBsAg-specific cellular immune responses 2 months after the third injection of HBsAg-pulsed DC were detected in patient 1 (Fig. 4).

DISCUSSION

Potent antiviral and antitumour effects of antigen-pulsed DC have been documented in animal models of human diseases since the 1980s. The first clinical trial of cancer antigen-pulsed DC was conducted in patients with cancer in 1996 [15]. Several clinical trials with cancer antigen-pulsed DC are ongoing worldwide [13]. It is expected that viral antigen-pulsed DC may be an effective immune therapy in patients with chronic viral infections, but such approaches have not yet been attempted clinically.

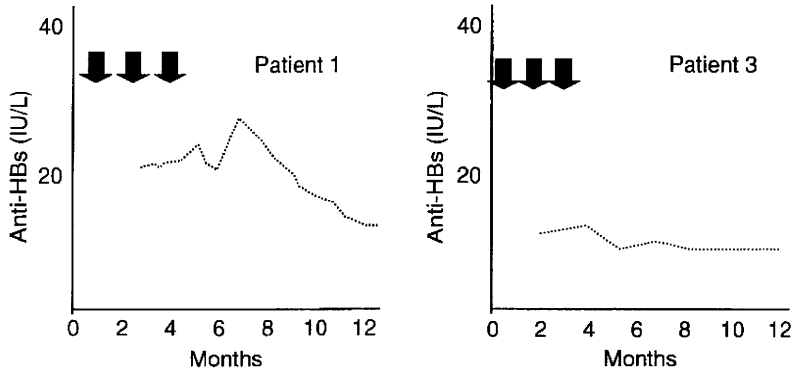

Fig. 3 Anti-HBs in 2 patients with chronic hepatitis B (CHB) after administration (arrows) of HBsAg-pulsed DC.

To treat patients with cancer, DC have been loaded with tumour-associated antigens, crude tumour products, tumour RNA, and other tumour-derived products *in vitro* [13,16]. The resultant cancer antigen-pulsed DC have been injected into patients with cancer, especially in those with advanced cancer. Many of these patients were immune compromised because they were in terminal stage of cancer. However, almost all patients with chronic viral infections are immune competent. Thus, a systemic and cautious approach is needed to prepare viral antigen-pulsed DC and initiate a clinical trial.

In this study, we used HBsAg, a well-known protein of HBV, to load human blood DC. As the safest source of HBsAg, we used a prophylactic hepatitis B vaccine. We showed that there was no free HBsAg in HBsAg-pulsed DC. This is important because if free antigen is present in HBsAg-pulsed DC, it will be difficult to assess the real effects of antigen-pulsed DC *in vivo* because free HBsAg may also induce immune responses *in vivo*. We also found that HBsAg-pulsed DC produced significantly higher levels of IL-12 and IFN-γ, two immune stimulatory cytokines compared to unpulsed DC. Furthermore, we checked for any contamination in HBsAg-pulsed DC. When we reproducibly produced immunogenic HBsAg-pulsed DC without any contamination, we moved forward to conduct this pilot study.

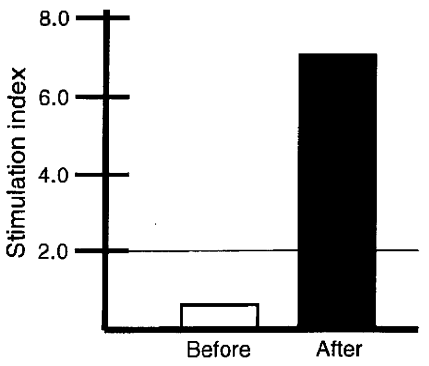

Fig. 4 HBsAg-specific cellular immune responses were seen after the third immunization of HBsAg-pulsed DC in patient 1.

Antigen-specific humoral and cellular immune responses were detected in 2 and 1 patients, respectively, because of administration of HBsAg-pulsed DC. It is premature to comment about the therapeutic efficacy of HBsAg-pulsed DC in this study because this is a pilot study. Indeed, there are several opportunities to improve our protocol. As the safest form of HBsAg, we used HBsAg in an HB vaccine. This allowed us to use a maximum of 10 μg of HBsAg to maximize DC viability during preparation of HBsAg-pulsed DC. In the future, human consumable recombinant HBsAg in larger doses may be used for preparing antigen-pulsed DC. We used only 5 million HBsAg-pulsed DC, as this was the first clinical trial of this nature. In the future, a dose escalation study with HBsAg-pulsed DC should be conducted. In addition, the number of patients needs to be increased.

Our study represents an initial effort to develop antigen-specific immune therapy for patients with CHB. We have systematically prepared HBsAg-pulsed DC and used them in normal volunteers [17] and hepatitis B vaccine nonresponders [14]. HBsAg-pulsed DC were completely safe and immunogenic in normal volunteers and hepatitis B vaccine nonresponders, who have been followed for 5 years after the administration of HBsAg-pulsed DC [14,17]. Finally, we used HBsAg-pulsed DC in patients with CHB and also confirmed the safety of this treatment. However, this is a small study, and there are several limitations that affect the interpretation of the findings. First, we only included five patients. In addition, patients were immunized 1–3 times with HBsAg-pulsed DC. However, this was a pilot study to demonstrate the use of DC-based therapy in immune competent persons with a chronic viral infection. We are now planning to prepare other HBV-related antigen-pulsed DC for patients with CHB because only HBsAg-pulsed DC may not be the best therapeutic option. Hepatitis B core antigen-pulsed DC may be required to restore therapeutic HBV-specific immunity. Also, antigen-pulsed DC may be used as a part of combination therapy with antiviral drugs in patients with CHB [18]. Finally, the concept and techniques used in this

study may be used to prepare antigen-pulsed DC for other chronic infections.

REFERENCES

1 Fattovich G. Natural history and prognosis of hepatitis B. *Semin Liver Dis* 2003; 23: 47–58.

2 Shamiliyan TA, MacDonald R, Shaukat A *et al.* Antiviral therapy for adults with chronic hepatitis B: a systemic review for a national institute of health consensus development conference. *Ann Intern Med* 2009; 150: 111–124.

3 Rehermann B. Immune responses to hepatitis B virus infection. *Semin Liver Dis* 2003; 23: 21–37.

4 Bertoletti A, Maini MK. Protection or damage: a dual role for the virus-specific cytotoxic T lymphocyte response in hepatitis B and C infection? *Curr Opin Microbiol* 2000; 3: 387–392.

5 Maini MK, Boni C, Lee CK *et al.* The role of virus-specific CD8(+) cells in liver damage and viral control during persistent hepatitis B virus infection. *J Exp Med* 2000; 191: 1269–1280.

6 Pol S, Driss F, Michel ML *et al.* Specific vaccine therapy in chronic hepatitis B infection. *Lancet* 1994; 344: 342.

7 Pol S, Nalpas B, Driss F *et al.* Efficacy and limitations of a specific immunotherapy in chronic hepatitis B. *J Hepatol* 2001; 34: 917–921.

8 Inchauspé G, Michel ML. Vaccines and immunotherapies against hepatitis B and hepatitis C viruses. *J Viral Hepat* 2007; 14(Suppl. 1): 97–103.

9 Steinman RM. Dendritic cells: understanding immunogenicity. *Eur J Immunol* 2007; 37(Suppl. 1): S53–S60.

10 Onji M, Akbar SM, eds. Dendritic Cells in Clinics. Tokyo: Springer, 2008.

11 Arima S, Akbar SMF, Michitaka K *et al.* Impaired function of antigen-presenting dendritic cells in patients with chronic hepatitis B: localization of HBV DNA and HBV RNA in blood DC by *in situ* hybridization. *Int J Mol Med* 2003; 11: 169–174.

12 van der Molen RG, Sprengers D, Binda RS *et al.* Functional impairment of myeloid and plasmacytoid dendritic cells of patients with chronic hepatitis B. *Hepatology* 2004; 40: 738–746.

13 Banchereau J, Paluka K. Dendritic cells as therapeutic vaccines against cancer. *Nature Rev Immunol* 2005; 3: 296–306.

14 Akbar SM, Furukawa S, Yoshida O *et al.* Induction of anti-HBs in HB vaccine nonresponders *in vivo* by hepatitis B surface antigen-pulsed blood dendritic cells. *J Hepatol* 2007; 47: 60–67.

15 Hsu FJ, Benike C, Fagnoni F *et al.* Vaccination of patients with B-cell lymphoma using autologous antigen-pulsed dendritic cells. *Nat Med* 1996; 2: 52–58.

16 Akbar SMF, Abe M, Yoshida M *et al.* Dendritic cell-based therapy as a multidisciplinary approach to cancer treatment: present limitation and future scopes. *Curr Med Chem* 2006; 13: 3113–3119.

17 Akbar SMF, Furukawa S, Onji M *et al.* Safety and efficacy of hepatitis B surface antigen-pulsed dendritic cells in human volunteers. *Hepatol Res* 2004; 29: 136–141.

18 Sprengers D, Janssen HL, Kwekkeboom J, Niesters HG, de Man RA, Schalm SW. *In vivo* immunization following virus suppression: a novel approach for inducing immune control in chronic hepatitis B. *J Viral Hepat* 2003; 10: 7–9.

Liver INTERNATIONAL
OFFICIAL JOURNAL OF THE INTERNATIONAL ASSOCIATION FOR THE STUDY OF THE LIVER

Liver International ISSN 1478-3223

CLINICAL STUDIES

Assessment of hepatic fibrosis by analysis of the dynamic behaviour of microbubbles during contrast ultrasonography

Hiroyuki Ishibashi, Hitoshi Maruyama, Masanori Takahashi, Keiichi Fujiwara, Fumio Imazeki and Osamu Yokosuka

Department of Medicine and Clinical Oncology, Chiba University Graduate School of Medicine, Inohana, Chuou-ku, Chiba, Japan

Keywords
contrast agent – fibrosis – liver – ultrasound

Correspondence
Hitoshi Maruyama, Department of Medicine and Clinical Oncology, Chiba University Graduate School of Medicine, 1-8-1, Inohana, Chuou-ku, Chiba, 260-8670, Japan
Tel: +81 43 226 2083
Fax: +81 43 226 2088
e-mail: maru-cib@umin.ac.jp

Received 11 March 2010
Accepted 24 June 2010

DOI:10.1111/j.1478-3231.2010.02315.x

Abstract

Background/aims: Microbubble behaviour from the portal vein to the liver parenchyma may reflect haemodynamic changes because of hepatic fibrosis. The aim of this study was to determine the efficacy of contrast-enhanced ultrasound (US) with Sonazoid™ for the assessment of the grade of hepatic fibrosis. *Methods:* This prospective study evaluated 117 patients with chronic liver disease (chronic hepatitis 85; cirrhosis 32) and 34 controls. All subjects received both contrast-enhanced US with Sonazoid™ for 1 min after the agent injection and subsequent liver biopsy. Flow velocity and flow volume in the right portal vein, onset time of contrast enhancement in the right hepatic artery and right portal vein, maximum intensity ratio between the intrahepatic portal vein and liver parenchyma, and time interval between the onset time and the time of maximum intensity ratio were compared with the pathological findings. *Results:* Among the evaluated parameters, time interval between the onset time and the time of maximum intensity ratio showed the closest relationship with the grade of hepatic fibrosis: 4.21 ± 1.32 for controls ($n = 34$), 5.58 ± 1.39 for F1 ($n = 31$), 6.79 ± 1.77 for F2 ($n = 28$), 8.85 ± 1.97 for F3 ($n = 26$) and 14.3 ± 3.49 for cirrhosis ($n = 32$); controls vs. F2, $P = 0.0004$; F1 vs. F3, $P < 0.0001$; F2 vs. F3, $P = 0.0177$; F3 vs. cirrhosis, $P < 0.0001$. The areas under the receiver operating characteristic curves of the time interval were 0.94, 0.96 and 0.98 for the diagnosis of marked fibrosis ($\geq$F2), advanced fibrosis ($\geq$F3) and cirrhosis respectively. *Conclusions:* Contrast-enhanced US with Sonazoid™ may be a promising method for the indirect evaluation of hepatic fibrosis.

Chronic liver disease is increasing in prevalence worldwide and is one of the most important clinical problems because it is a high-risk factor for the development of portal hypertension and hepatocellular carcinoma (1–3). The severity of chronic liver disease depends on the grade of hepatic fibrosis, whose assessment supports the clinical management of these patients (4, 5). Liver biopsy remains the gold standard for the evaluation of the grade of hepatic fibrosis, in spite of its invasiveness in patients with impaired coagulation (6, 7) and the possibility of sampling error because of the heterogeneous distribution of fibrosis (8). Because patients with chronic liver disease require long-term follow-up, a repeatedly available noninvasive method is preferable for the assessment of hepatic fibrosis (9–12).

Thanks to its noninvasiveness and convenience, ultrasound (US) is one of the procedures applied most frequently for the periodic evaluation of diffuse liver disease. However, as the diagnostic accuracy of US for cirrhosis is not high, it is not regarded as a reliable method for the evaluation of the grade of hepatic fibrosis (11, 12). In recent times, the development of microbubble contrast agents has increased the diagnostic capability of US, and harmonic imaging with second-generation contrast agents confers a stable enhancement effect in the liver with improved signal-to-noise ratio (13–17). Analysis of the dynamic behaviour of microbubbles may enable a noninvasive evaluation of the severity of chronic liver disease (18–21).

Hepatic fibrosis in the downstream area may affect the inflow haemodynamics of the upstream portal vein, and the behaviour of microbubbles between the portal vein and liver parenchyma may reflect the vascular resistance, according to the grade of hepatic fibrosis. On this basis, we measured the changes of intensity ratio between the intrahepatic portal vein and liver parenchyma during contrast enhancement with Sonazoid™ (13, 15, 17) and compared the results with the histological grade of fibrosis in patients with chronic hepatitis or cirrhosis, and control subjects. The aim of this study was to determine the efficacy of contrast-enhanced US with Sonazoid™ for the assessment of the grade of hepatic fibrosis.

Patients and methods

Patients

This prospective study was carried out in our department from December 2007 to December 2009. The inclusion criteria for patients were as follows: (i) chronic liver disease patients without history or clinical signs of liver tumour, (ii) patients for whom liver biopsy was scheduled. Healthy volunteers without signs of liver disease were evaluated as controls. The exclusion criteria for all the participants included the presence of liver tumours, portal vein thrombus or vascular abnormalities such as reversed flow, arterio-portal communication or obstruction, use of vasoactive drugs, significant alcohol consumption (> 20 g/day) within 2 months, pregnancy and the presence of egg allergy, which is a contraindication of Sonazoid™ (GE Healthcare, Oslo, Norway).

There were 161 participants: 127 patients with chronic liver disease (54 males, age 50.2 ± 13.7 years, 26–78; 73 females, age 56.2 ± 11.2 years, 23–76) and 34 controls (17 males, age 48.2 ± 16.9 years, 26–82; 17 females, age 53.5 ± 17.5 years, 25–85). The 127 patients underwent liver biopsy; however, the specimens were inadequate for fibrosis staging in 7 (5.5%) of them. US examination before contrast-enhanced US detected focal hepatic lesions in two patients and a portal vein thrombus in one patient. Therefore, 10 patients were excluded and the remaining 151 subjects were the participants in this study. There were 85 patients with chronic hepatitis (34 males, age 49.4 ± 15.2 years, 26–78; 51 females, age 55.9 ± 10.8 years, 23–73) and 32 patients with cirrhosis (12 males, age 55.5 ± 12.7 years, 37–75; 20 females, age 64.9 ± 8.04 years, 46–76). The mean body mass index of all subjects was 22.9 ± 3.78 kg/m^2 (16–37). Seventeen patients with cirrhosis were classified as Child–Pugh grade A and 15 were classified as grade B. The causes of chronic liver disease were as follows: viral in 90 patients (hepatitis C virus in 74 and hepatitis B virus in 16), alcohol abuse in six patients, nonalcoholic steatohepatitis in nine patients, autoimmune hepatitis in eight patients, primary sclerosing cholangitis in one patient and cryptogenic in three patients. Laboratory tests, including aspartate transaminase (AST, IU/L), alanine transaminase (ALT, IU/L) and platelet count (10^9/L), were carried out on all subjects to calculate the APRI (AST/35 × 100/platelet count) and FIB4 [age × AST/(platelet count × ALT$^{0.5}$)] as indirect markers of fibrosis (Table 1) (22).

The study protocol was in accordance with the Declaration of Helsinki and was approved by the ethics committee of our department. Informed written consent was obtained from all participants.

Ultrasound examination

The equipment was AplioXG (Toshiba, Tokyo, Japan) with a 3.75 MHz convex probe. US examinations were performed under the supine position with more than 4-h fasting.

Firstly, noncontrast grey-scale US was carried out to screen for focal hepatic lesions or portal vein thrombi. Then, colour Doppler US was performed to determine the presence or absence of vascular abnormalities. Next, a scan plane for the right lobe of the liver was selected to observe the main branch of the intrahepatic right portal vein and the right hepatic artery. Pulsed Doppler US was performed to measure the mean flow velocity and mean flow volume of the right portal vein. Sampling width was set according to the diameter of the vessel, and the angle between the US beam and the vessel was equal to or < 60° in all measurement procedures.

After that, contrast-enhanced US was performed with harmonic imaging (15 Hz) under the low mechanical index of 0.25, which has been used for Sonazoid™ in a published study (17). The depth was set to cover the entire right lobe of the liver, with a focus point 8 cm below the skin surface under right intercostal scan. Gain was adjusted at an optimal level and the dynamic range was set at 55 dB.

We injected the contrast agent Sonazoid™ (0.0075 ml/kg) manually into the antecubital vein at a rate of 1.0 ml/s, followed by a 3.0 ml flush of normal saline, and immediately started the chronometer of US equipment. The participants were asked to breathe shallowly and gently after the injection. Contrast-enhanced sonograms were taken for 1 min after the agent injection and all the cine images were recorded digitally on the hard disc of the US system.

Table 1. Clinical and biochemical data of subjects

	Controls, $n = 34$	Chronic hepatitis, $n = 85$	Cirrhosis, $n = 32$	P
Age, years	50.9 ± 17.1 (25–85)	53.3 ± 13.1 (23–78)	61.4 ± 10.9 (37–76)	0.01
Gender, male/female	17/17	34/51	12/20	0.56
Body mass index, kg/m^2	21.7 ± 2.78 (18–27)	23.2 ± 3.87 (16–34)	24.1 ± 4.45 (16–37)	0.04
HCV/HBV/alcohol/NASH/AIH/PSC/cryptogenic	–	60/15/0/5/5/0/0	14/1/6/4/3/1/3	
Presence of ascites	–	–	6	
Platelet count, 10^9/L	245 ± 49.5 (163–340)	188 ± 51.7 (97.0–335)	117 ± 91.0 (44.0–430)	< 0.01
APRI	0.23 ± 0.08 (0.11–0.52)	1.03 ± 1.00 (0.20–5.70)	1.76 ± 1.02 (0.33–5.07)	< 0.01
FIB4	1.02 ± 0.56 (0.30–2.57)	2.22 ± 1.53 (0.39–7.90)	6.40 ± 3.32 (1.04–13.2)	< 0.01
Histological staging, F0/F1/F2/F3/cirrhosis	–	0/31/28/26/0	0/0/0/0/32	
Child-Pugh grade, A/B/C	–	–	17/15/0	

AIH, autoimmune hepatitis; ALT (IU/L), alanine transaminase; APRI, (AST/35) × 100/platelet count; AST (IU/L), aspartate transaminase; FIB4, age × AST/(platelet count/ALT$^{0.5}$); HBV, hepatitis B virus; HCV, hepatitis C virus; NASH, nonalcoholic steatohepatitis; PSC, primary sclerosing cholangitis.

The US operators were HI in all 151 subjects and MT in 17 subjects of them, both with a 7-year experience of US examination. Inter-observer variability was examined in 17 subjects (controls five, chronic hepatitis three, cirrhosis nine), with the second US examination being performed within 7 days (3.6 ± 2.3) of the initial examination. Intra-observer variability by operator HI was examined in 10 subjects (controls two, chronic hepatitis four, cirrhosis four), with the second US examination being performed within 6 days (2.6 ± 1.9) of the initial examination. The results of the second US examination were used only to measure inter- or intra-observer variability. Clinical symptoms and vital signs of blood pressure, heart rate and oxygen saturation were checked before and after US examinations.

Liver biopsy and pathological examination

One hundred and seventeen patients (chronic hepatitis 85, cirrhosis 32) received liver biopsy within a week of the contrast-enhanced US examination. Biopsy specimens were obtained by percutaneous needle biopsy (16 G needle; BARD, Tempe, AZ, USA) in 111 patients without ascites and transjugular liver biopsy (18 G needle; Cook, Bloomington, IN, USA) in six patients with ascites. Paraffin-embedded specimens were stained with haematoxylin–eosin and Azan. Two experienced hepatologists (F. I., K. F.) evaluated the fibrosis stage according to the staging scoring system recommended by Desmet *et al.* (4) and Scheuer (7).

Data analysis

Contrast analysis was performed using an off-line personal computer with IMAGELAB-AVI software (Toshiba, Tokyo, Japan) by H. M., who was not an operator of US and was not aware of any information regarding the subjects. Firstly, we observed the cine images with frame-by-frame playback to find the first frame showing the arrival of the contrast agent in the right hepatic artery or right portal vein. The time between the agent injection and the first frame of contrast arrival in each vessel was defined as the onset time of contrast enhancement, which may reflect the extrahepatic haemodynamics of microbubbles (Fig. 1). Then, we prepared two circular regions of interest in the liver at the same depth: one for the right portal vein and the other for liver parenchyma. These two regions of interest, which were of an equal diameter, were set manually on the series of successive images for 1 min with frame-by-frame advance for analysis after the exclusion of inappropriate, blurred images (Fig. 2). Automatic calculation of the intensity ratio between the right portal vein and liver parenchyma in each frame provided a time-related intensity ratio curve featuring the intrahepatic haemodynamics of the microbubbles. The maximum intensity ratio between the right portal vein and liver parenchyma, and time interval from the onset of contrast enhancement in the right portal vein to the time of the maximum intensity ratio between the right portal vein and liver parenchyma were measured on this curve (Fig. 3). Inter- and intra-observer variability of measured parameters was calculated from the coefficient of variation obtained by standard deviation/mean $\times$ 100.

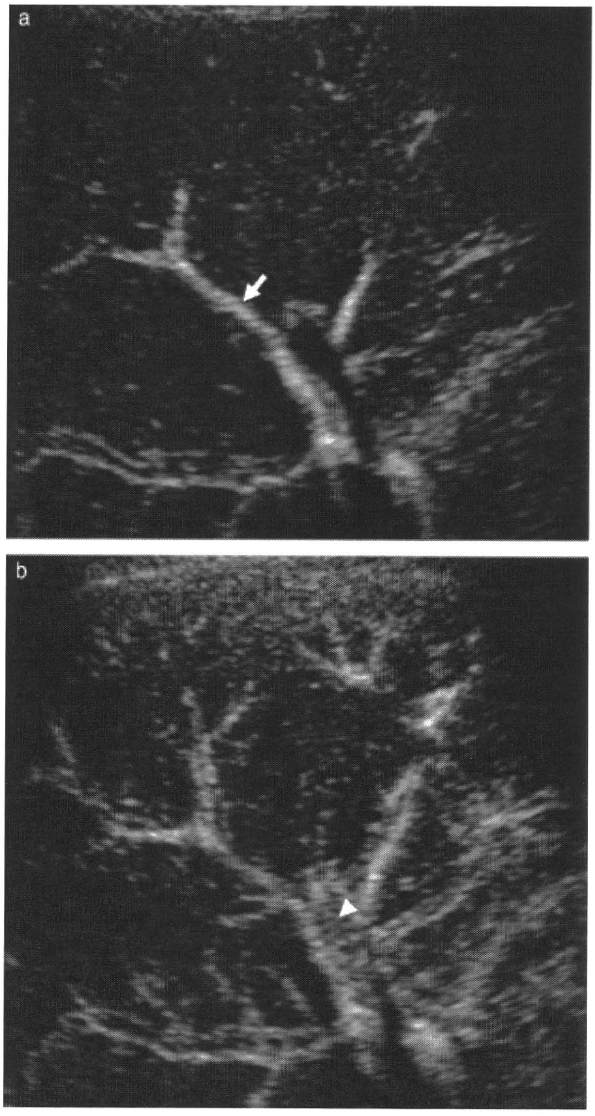

Fig. 1. Contrast-enhanced ultrasound images under right intercostal scan. (a) Onset time of contrast enhancement in the right hepatic artery: onset time of contrast enhancement was 14 s after the injection of Sonazoid™ in the right hepatic artery (arrow). (b) Onset time of contrast enhancement in the right portal vein: onset time of contrast enhancement was 16 s after the injection of Sonazoid™ in the right portal vein (arrowhead).

Statistical analysis

All data were expressed as mean $\pm$ standard deviation, range or percentage. Comparison of age, body mass

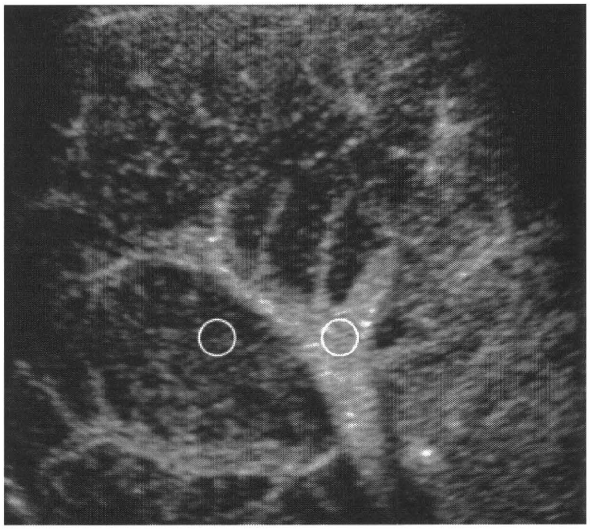

Fig. 2. Measurement of the intensity in the right portal vein and liver parenchyma. Two circular regions of interest were set on the right portal vein and adjacent liver parenchyma at the same depth.

index, platelet count, APRI, FIB4, mean flow velocity and mean flow volume in the right portal vein, onset time of contrast enhancement in the right hepatic artery and right portal vein, the maximum intensity ratio between the right portal vein and liver parenchyma, and the time interval from the onset of contrast enhancement in the right portal vein to the time of the maximum intensity ratio, with the grade of fibrosis was performed by analysis of variance using the Scheffe *post hoc* test. The χ^2-test was used to compare the gender in three groups (controls, chronic hepatitis and cirrhosis). Areas under the receiver operating characteristic curves (AUC) with 95% confidence interval were calculated for the prediction of marked fibrosis ($\geq$F2), advanced fibrosis ($\geq$F3) and cirrhosis in the time interval from the onset of contrast enhancement in the right portal vein to the time of the maximum intensity ratio, FIB4 and APRI. Sensitivity, specificity, positive predictive value, negative predictive value and diagnostic accuracy were calculated for the best cut-off values obtained for each fibrosis stage. Probability values < 0.05 were considered to be significant. All statistical analyses were performed using the SPSS package (version 17.0J; SPSS, Chicago, IL, USA). AUC were obtained using ROCKIT1.1B2 (23).

Results

Results of liver biopsy

The mean length of the liver biopsy specimens was 21.6 ± 3.51 (15–25) mm, and the number of portal tracts was 13.5 ± 4.61 (11–30). The fibrosis stages by the consensus reading of results were F0 in 0 (0%), F1 in 31 (26.5%), F2 in 28 (23.9%), F3 in 26 (22.2%) and cirrhosis in 32 (27.4%) (Table 1).

Blood flow measurement in the right portal vein

The mean flow velocity (cm/s) of the right portal vein was 11.4 ± 2.04 (7.90–19.3) in controls, 10.4 ± 1.94 (5.90–15.1) in chronic hepatitis and 8.96 ± 1.84 (5.50–13.3) in cirrhosis. The mean flow volume (ml/min) of the right portal vein was 342 ± 101 (160–820) in controls, 318 ± 114 (100–760) in chronic hepatitis and 295 ± 136 (90.0–710) in cirrhosis. There were significant differences in mean flow velocity (controls vs. chronic hepatitis, $P = 0.0259$; controls vs. cirrhosis, $P < 0.0001$; and chronic hepatitis vs. cirrhosis, $P = 0.0113$), showing no significant differences among F1, F2 and F3. There were no significant differences in mean flow volume among controls, chronic hepatitis and cirrhosis ($P = 0.3134$). Interobserver variability was 10% for mean flow velocity and 15% for mean flow volume, and intra-observer variability was 8.7% for mean flow velocity and 14% for mean flow volume.

Relationship between the parameters of contrast enhancement and the degree of hepatic fibrosis

The onset time of contrast enhancement in the right hepatic artery was 14.3 ± 2.22 s (11–21) in controls, 15.0 ± 3.22 s (9–24) in chronic hepatitis and 14.1 ± 3.15 s (6–23) in cirrhosis and that in the right portal vein was 16.9 ± 2.44 s (13–22) in controls, 18.4 ± 3.96 s (12–29) in chronic hepatitis and 18.3 ± 3.39 s (8–26) in cirrhosis. There were no significant differences in the onset time of contrast enhancement in the right hepatic artery and right portal vein among the three groups (Fig. 4). The maximum intensity ratio between the right portal vein and liver parenchyma was 22.2 ± 5.84 dB (12–34) in controls, 19.2 ± 4.66 dB (13–32) in F1, 17.8 ± 3.73 dB (6–24) in F2, 16.1 ± 5.27 dB (8–30) in F3 and 13.8 ± 5.34 dB (3–21) in cirrhosis (controls vs. F2, $P = 0.0219$; controls vs. F3, $P = 0.0005$; controls vs. cirrhosis, $P < 0.0001$; F1 vs. cirrhosis, $P = 0.0023$) (Fig. 5). The time interval from the onset of contrast enhancement in the right portal vein to the time of the maximum intensity ratio was 4.21 ± 1.32 s (1–7) for controls, 5.58 ± 1.39 s (2–10) for F1, 6.79 ± 1.77 s (4–13) for F2, 8.85 ± 1.97 s (6–14) for F3 and 14.3 ± 3.49 s (9–21) for cirrhosis, and significant differences were found between controls and F2 ($P = 0.0004$), F1 and F3 ($P < 0.0001$), F2 and F3 ($P = 0.0177$), and F3 and cirrhosis ($P < 0.0001$) (Fig. 3). Six patients with ascites were diagnosed with cirrhosis by biopsy specimens obtained and their time interval from the onset of contrast enhancement in the right portal vein to the time of the maximum intensity ratio was 12.2 ± 2.40 s (10–14). Inter-/intra-observer variability was 6.1%/5.5% for onset time of contrast enhancement in the right hepatic artery, 7.1%/6.7% for onset time of contrast enhancement in the right portal vein, 7.5%/7.2% for the maximum intensity ratio between the right portal vein and liver parenchyma and 6.0%/5.7% for the time interval from the onset of contrast enhancement in the right portal vein to the time of the maximum intensity ratio. No adverse effect was observed during and after the US examination.

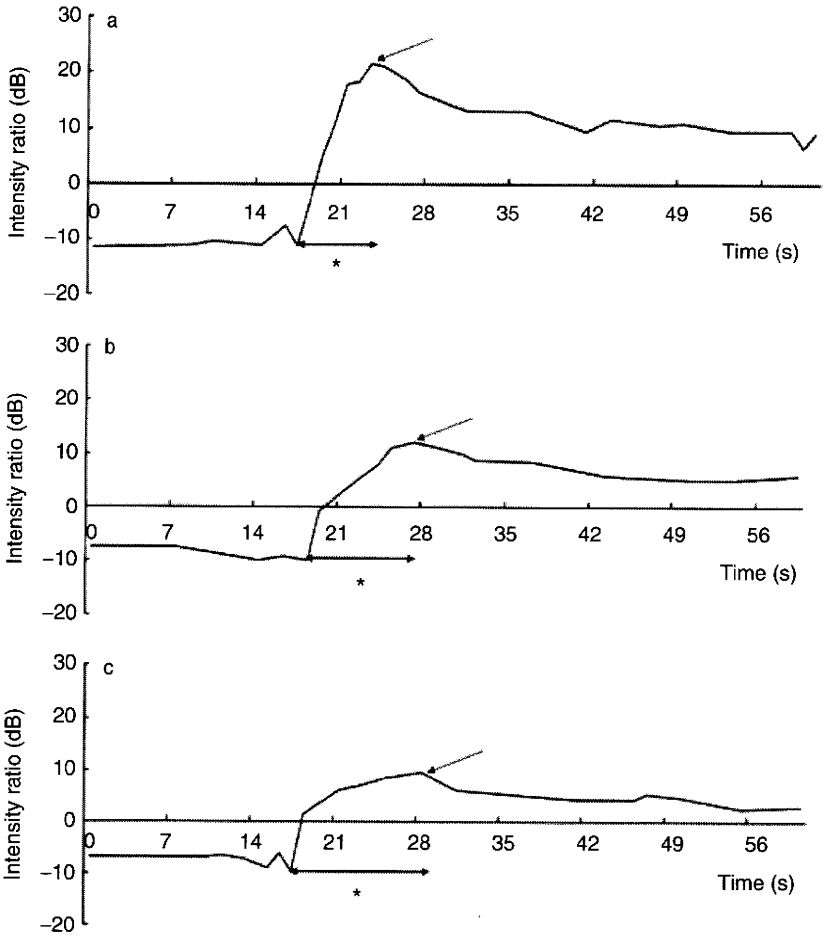

Fig. 3. Time-related changes in intensity ratio between the right portal vein and liver parenchyma. (a) Control subject (56 years old, female): the maximum intensity ratio between the right portal vein and liver parenchyma was 22 dB and time interval from the onset of contrast enhancement in the right portal vein to the time of the maximum intensity ratio was 6 s. (b) Patient with chronic hepatitis (52 years old, female, hepatitis C virus, F3): the maximum intensity ratio between the right portal vein and liver parenchyma was 13 dB and time interval from the onset of contrast enhancement in the right portal vein to the time of the maximum intensity ratio was 9 s. (c) Patient with cirrhosis (56 years, female, hepatitis C virus): the maximum intensity ratio between the right portal vein and liver parenchyma was 9 dB and time interval from the onset of contrast enhancement in the right portal vein to the time of the maximum intensity ratio was 12 s. Arrow, maximum intensity ratio between the right portal vein and liver parenchyma.
*Time interval from the onset of contrast enhancement in the right portal vein to the time of the maximum intensity ratio between the right portal vein and liver parenchyma.

Diagnostic value of time interval from the onset of contrast enhancement in the right portal vein to the time of the maximum intensity ratio for the grade of fibrosis

The AUC of the time interval from the onset of contrast enhancement in the right portal vein to the time of the maximum intensity ratio were 0.94 (0.89–0.97) for marked fibrosis with the best cut-off value of 6.5 s, 0.96 (0.93–0.98) for advanced fibrosis with the best cut-off value of 8 s and 0.98 (0.95–0.99) for cirrhosis with the best cut-off value of 9.5 s. Six patients with ascites had a time interval from 10 to 14 s, which ranged over the best cut-off value. These AUC values were significantly higher than those of APRI and FIB4: 0.86 (0.79–0.92) and 0.85 (0.79–0.91) for marked fibrosis, 0.85 (0.78–0.90) and 0.89 (0.82–0.94) for advanced fibrosis and 0.80 (0.71–0.86) and 0.90 (0.82–0.95) for cirrhosis respectively (Table 2, Fig. 6). Sensitivity, specificity, positive predictive value, negative predictive value and diagnostic accuracy were 84, 88, 84, 88 and 87% for marked fibrosis, 83, 93, 89, 90 and 89% for advanced fibrosis and 95, 92, 77, 98 and 93% for cirrhosis respectively.

Discussion

The present study revealed that the maximum intensity ratio between the right portal vein and liver parenchyma